Remote Sensing of Environment 146 (2014) 11–23

Contents lists available at ScienceDirect

Remote Sensing of Environment

journal homepage: www.elsevier.com/locate/rse

Combining model and geostationary satellite data to reconstruct hourly SST field over the Mediterranean Sea

S. Marullo [a,*], R. Santoleri [b], D. Ciani [b], P. Le Borgne [c], S. Péré [c], N. Pinardi [d], M. Tonani [e], G. Nardone [f]

[a] Agenzia nazionale per le nuove tecnologie, l'energia e lo sviluppo economico sostenibile, ENEA — Centro Ricerche Frascati, Frascati, Italy
[b] CNR — Istituto di Scienze del'Atmosfera e del Clima, Rome, Italy
[c] Meteo-France/DP/CMS, Lannion, France
[d] Department of Physics and Astronomy, University of Bologna, Italy
[e] Istituto Nazionale di Geofisica e Vulcanologia, Bologna, Italy
[f] Istituto Superiore per la Protezione e la Ricerca Ambientale (ISPRA), Italy

ARTICLE INFO

Article history:
Received 1 November 2012
Received in revised form 8 November 2013
Accepted 10 November 2013
Available online 2 December 2013

Keywords:
Sea Surface Temperature
Mediterranean
Diurnal Cycle
Geostationary Satellite
Model

ABSTRACT

This work focuses on the reconstruction of Sea Surface Temperature (SST) diurnal cycle through combination of numerical model analyses and geostationary satellite measurements. The approach takes advantage of geostationary satellite observations as the diurnal signal source to produce gap-free optimally interpolated (OI) hourly SST fields using model analyses as first-guess. The resulting SST anomaly field (satellite-model) is free, or nearly free, of any diurnal cycle, thus allowing one to interpolate SST anomalies using satellite data acquired at different times of the day.

The method is applied to reconstruct the hourly Mediterranean SST field during summer 2011 using SEVIRI data and Mediterranean Forecasting System analyses. A synthetic cloud reconstruction experiment demonstrated that the OI SST method is able to reconstruct an unbiased SST field with a RMS = 0.16 °C with respect to SEVIRI observations. The OI interpolation estimate, the model first guess and the SEVIRI data are evaluated using drifter and mooring measurements. Special attention is devoted to the analysis of diurnal warming (DW) events that are particularly frequent in the Mediterranean Sea. The model reproduces quite well the Mediterranean SST diurnal cycle, except for the DW events. Due to the thickness of the model surface layer, the amplitude of the model diurnal cycle is often less intense than the corresponding SEVIRI and drifter observations. The Diurnal OI SST (DOISST) field, resulting from the blending of model and SEVIRI data via optimal interpolation, reproduces well the diurnal cycle including extreme DW events. The evaluation of DOISST products against drifter measurements results in a mean bias of −0.07 °C and a RMS of 0.56 °C over interpolated pixels. These values are very close to the corresponding statistical parameters estimated from SEVIRI data (bias = −0.16 °C, RMS = 0.47 °C). Results also confirm that part of the mean bias between temperature measured by moorings at 1 m depth and the satellite observations can be ascribed to the different nature of the measurements (bulk versus skin).

1. Introduction

The precise knowledge of the Sea Surface Temperature (SST) is extremely important for many environmental applications. In fact, not only is SST a key variable that modulates air–sea heat exchanges, but it also plays a key role in many biological and chemical processes within the upper ocean.

A wide variety of in situ SST measurements, acquired by drifting or moored buoys, Conductivity, Temperature and Depth (CTD), expendable bathythermograph (XBT), and underwater data logger ship measurements, provide data at depths ranging from a few millimeters to several meters. These measurements, even when acquired with high temporal resolution, have limited spatial coverage and often limited temporal duration. Satellite observations can actually contribute to mitigate these limitations by providing synoptic information when in situ data are scarce or absent.

Since the pioneering work of Anding and Kauth (1970) and Prabhakara, Dalu, and Kunde (1974) the accuracy of SST retrieval from some satellite sensors has improved from a few degree Celsius to less than or of the order of a few tenths. In recent years, the Advanced Along Track Scanning Radiometer on Envisat achieved an accuracy of 0.1–0.3 °C (Embury, Merchant, & Corlett, 2012).

This accuracy range is the one required by the Regional Coupled Models (RegCM) and Ocean Models (Intergovernmental Oceanographic

* Corresponding author at: Agenzia nazionale per le nuove tecnologie, l'energia e lo sviluppo economico sostenibile, ENEA — Centro Ricerche Frascati, Via E. Fermi 45, 00044 Frascati, Italy. Tel.: +39 0694005867.
E-mail address: salvatore.marullo@enea.it (S. Marullo).

0034-4257/$ – see front matter © 2013 Elsevier Inc. All rights reserved.
http://dx.doi.org/10.1016/j.rse.2013.11.001

Commission, 1999) and it is also comparable to, or lower than, typical amplitudes of the diurnal cycle (Fig. 2 of Kennedy, Brohan, & Tett, 2007). The present-day accuracy of the satellite SST retrieval allows one to resolve the typical day–night SST excursions. This SST excursion can also reach values over 3 °C as regularly observed in the world oceans under low-wind and strong solar heating conditions (Gentemann, Minnett, Le Borgne, & Merchant, 2008; Jessup & Branch, 2008; Merchant et al., 2008; Minnett, 2003; Stommel, 1969; Stommel & Woodcock, 1951).

The SST diurnal cycle has many implications on mixed layer dynamics and on the air–sea fluxes. Chen and Houze (1997) showed that the SST diurnal cycle can be related to the evolution of convective clouds over the Tropical Warm Pool. This area exhibits widespread occurrences of high SST diurnal warming events, with some extreme events measured from MODIS and MTSAT-1R skin SST data exceeding 5 °C over small spatial/time scales (see https://www.ghrsst.org/ghrsst-science/science-team-groups/dv-wg/twp/). In the Tropical Pacific, the SST diurnal cycle triggers cloud convection when SST reaches its maximum value, typically around 14:00–15:00 Local Solar Time (LST in the following). Moreover Zeng and Dickinson (1998) studied SST diurnal variations and their impact on the numerical modeling of heat fluxes. They first analyzed data from TOGA TAO moored buoys in the Tropical Pacific, finding that the latent heat flux clearly shows diurnal amplitudes up to 20 W/m^2 on a monthly average. Introducing hourly (instead of daily or monthly averaged) SST values in a numerical model of latent and sensible heat fluxes, they found an offset in the modeled fluxes up to 10 W/m^2.

These results and requirements imply that the existence of a diurnal SST cycle cannot be neglected any more when using satellite SST data acquired at different times of the day. Moreover, recent findings indicate that the inclusion of sub-daily frequencies in the coupling of ocean and atmospheric models can have a significant impact in producing a more realistic spatial pattern of warming and precipitation in the Tropical Pacific (Bernie et al., 2008), or it can increase the intraseasonal SST response to the Madden–Julian Oscillation by 20% and the intensity of Ekman cells and equatorial upwelling by 10% (Bernie, Guilyardi, Madec, Slingo, & Woolnough, 2007).

Satellite infrared measurements can be interpreted directly in terms of the skin temperature (i.e. the temperature of the first few microns of the ocean surface, Casey, Donlon, & GHRSST Science Team, 2011). This quantity can only be measured in situ by radiometers rather than by conventional instruments operating from buoys or ships that can only provide the so-called bulk-temperature at depths varying from a few centimeters to several meters. Hence, satellite skin SST and bulk SST cannot be considered to be the same quantity, and their differences need to be interpreted in the light of the physical processes that occur in the upper ocean and at the air–sea interface (Zeng & Beljaars, 2005; Zeng, Zhao, Dickinson, & He, 1999).

On average, the difference between skin and bulk temperature is about −0.2 °C at night but can also reach several degrees during the day under favorable diurnal wind and heating conditions (Gentemann & Minnett, 2008). In this sense, satellite SST, even when obtained using retrieval methods based on regressions against in situ bulk temperature measurements, must be thought as a skin temperature adjusted to the skin-to-bulk mean bias. This implies that satellite SSTs will vary in time with the same frequency as a skin SST even though the day–night amplitude difference of the skin satellite SST can be biased by the day and night regression algorithms.

For several applications the availability of the skin rather than the bulk temperature is not a limitation. In fact the radiative, latent, and sensible heat exchanges between the ocean and the atmosphere depend on the actual skin temperature. Webster, Clayson, and Curry (1996), by using data acquired during the TOGA COARE IOP (Intensive Observing Period) (Webster & Lukas, 1992), have shown that a 1 °C variation in SST can produce changes in upwelling longwave, sensible heat and latent heat fluxes of 1.3%, 23.3% and 16.2%, respectively. These changes are all of the same sign and they result in a net change in the total heat fluxes. In the Mediterranean, diurnal SST variations can easily exceed the Tropical Pacific values (Merchant et al., 2008), so that their effect cannot be neglected.

A work dating back to 2003 (Stuart-Menteth, Robinson, & Challenor, 2003), investigates diurnal SST oscillations on a global scale by means of Advanced Very High Resolution Radiometer (AVHRR) satellite measurements. In particular, the frequency of oscillations greater than 0.5 °C in summer during July for several years has been checked. The authors showed that, compared to the Global Ocean, the Mediterranean Sea and the Mid-Atlantic are the regions of the Global Ocean where such important diurnal oscillations are more frequent.

A recent report by Sykes, While, Sellar, and Martin (2011) has correctly noted that, in order to resolve the diurnal cycle, satellite SST must be both sufficiently accurate to measure the diurnal signal and frequent enough to capture the diurnal variability. The Nyquist sampling theorem (Nyquist, 1924) imposes a sampling rate higher than twice per day to reconstruct a purely sinusoidal diurnal cycle. Since the SST diurnal cycle is not a perfect sinusoidal function at least 4 samples per day are needed to describe it properly (Sykes et al., 2011). In principle, geostationary satellites can sample the SST with enough frequency to resolve the diurnal cycle when cloud cover is not too persistent. Sykes et al. (2011) verified that, in the region covered by SEVIRI the diurnal cycle is sampled sufficiently for only half of the possible days but, fortunately, the Mediterranean Sea appears more sampled than any other area of the world ocean. These last considerations make the Mediterranean Sea one of the best areas to investigate a new methodology for reconstructing the diurnal cycle spatial and temporal variability on the basis of the available SST measurements from geostationary satellites.

The aim of this paper is to evaluate the capability of SEVIRI to resolve the diurnal SST variability in the Mediterranean Sea and reconstruct the hourly SST field under cloudy pixels. The reconstruction is operated by means of an upgraded version of the Diurnal Optimal Interpolation (DOI) scheme proposed by Marullo, Santoleri, Banzon, Evans, and Guarracino (2010). This approach was designed specifically for the tropical Atlantic region, taking into account the characteristic meteorological and oceanic time scales, as well as duration of the day and availability of satellite data for that study area. The same authors pointed out the need to investigate the problems of reconstructing the diurnal cycle in regions toward middle and high latitudes, where environmental conditions and scales involved in the SST variability are different. The approach we propose here makes use of observational and numerical model data in order to improve on the exclusively observational approach proposed by Marullo et al. (2010). The new DOI scheme (Section 3), proposed in this paper, uses hourly SST produced by the Mediterranean Forecasting System—MFS (Dobricic et al., 2007; Oddo et al., 2009; Pinardi & Coppini, 2010) as first-guess and the satellite observations to generate hourly interpolated SST fields. The analysis is focused on summer 2011 (June to August) in order to include the very frequent diurnal warming (DW) events, typical of the Mediterranean summer, which can produce abrupt changes in the SST oscillation. At present, MFS uses only the nighttime satellite data to correct the air–sea fluxes in the model via a flux correction algorithm applied once a day (Dobricic et al., 2007). The new method is a step toward the implementation of an assimilation scheme that aims to use the hourly SEVIRI dataset to correct the model diurnal cycle inaccuracies.

The evaluation of the proposed DOI method (Section 4) includes: 1) classical validation to verify whether the satellite estimates and analysis reconstruction are accurate enough to capture diurnal variations and correctly reproduce the intense diurnal warming events as seen by satellite; 2) spectral analysis to verify whether the satellite sampling is frequent enough to capture the diurnal variability also considering the unavoidable presence of data gaps.

2. The data

2.1. Satellite data

The satellite data used in this work are hourly nighttime and daytime SST fields acquired by the Spinning Enhanced Visible and Infra-Red Imager (SEVIRI) onboard Meteosat Second Generation (MSG), covering the summer 2011 from June 1st to August 31st. These data have been produced operationally by the European Organisation for the Exploitation of Meteorological Satellites (EUMETSAT) Ocean and Sea Ice Satellite Application Facility (OSI-SAF) at Météo-France/Centre de Météorologie Spatiale (CMS) in Lannion (EUMETSAT, 2011). The SEVIRI SST has been derived from METEOSAT-9 brightness temperatures using a nonlinear split window algorithm (NLSST, Walton, Pichel, Sapper, & May, 1998). A Numerical Weather Prediction (NWP) model-derived correction is added to the NLSST, according to Le Borgne, Roquet, and Merchant (2011). SEVIRI SSTs are skin SSTs adjusted to nighttime buoy measurements by adding a simple constant that does not vary after the first months of operations (François, Brisson, Le Borgne, & Marsouin, 2002; Merchant & Le Borgne, 2004). In the practical case of METEOSAT-9 corresponding to this study, the constant has been determined in 2006 and has been applied unchanged since then. This defines OSI-SAF SST as subskin temperature (by day and night), if needed, conversion to skin SST can be done by subtracting 0.2 °C to these values. The cloud mask used in the OSI-SAF SST chain is the EUMETSAT Nowcasting Satellite Application Facility (NWC-SAF) cloud mask developed by Derrien and Le Gléau (2005).

The hourly product (L3C) we used is the combination of all Meteosat acquisitions within 1 h, selecting, for each pixel, the best measure in terms of quality flags, rather than the average. Quality flags are represented by a scale of five levels: 5 = "excellent", 4 = "good", 3 = "acceptable", 2 = "bad", 1 = "erroneous". Quality flag for pixels where the calculation has not been attempted for other reasons (e.g. land) has a distinct confidence level 0, which means "unprocessed". For this specific work, we only retained SST data with quality flag greater than or equal to 4. This choice was the result of several trials and a good compromise between having as many data as possible, and the requirement to avoid any environmental contamination in our SST dataset.

These hourly SST products are made available in near real time (see www.osi-saf.org). Resolution varies in the SEVIRI disk, but is typically 5 km for the Mediterranean Sea.

2.2. In situ data

As skin temperature measurements were not available in the Mediterranean Sea during the investigation period, we used bulk measurements for the validation of the hourly satellite and the DOISST fields. The validation results are then discussed also in the light of the intrinsic difference between skin and bulk temperatures.

Moored buoys sea temperature data were obtained from the MyOcean Mediterranean in situ Thematic Assembly Center (MED INS-TAC) and the Italian network of wave stations, i.e. the ISPRA network. The MED INS-TAC and ISPRA networks contain the real-time in situ data for temperature and salinity measurements. The data are quality controlled using automated procedures and assessed using statistical analysis residuals. The spatial distribution of the MED INS-TAC and ISPRA moorings, with water temperature sensors installed, is shown in Fig. 1. Temperatures are recorded at several depths ranging from near surface (typically 1 m) to a few meters. For each mooring we selected the temperature sensor closest to the surface. Temperatures are available hourly or every half an hour for the Western Mediterranean sites and every 3 h for the Aegean Sea.

The drifter SST data used in this work are distributed via the GTS (Global Telecommunication System) and have been obtained from the MyOcean INS-TAC. The information on the quality of the data has been used to exclude suspect measurements, keeping only the highest quality data (for more details on the procedures adopted by the data producers see also the MyOcean in situ TAC Product User Manual, http://catalogue.myocean.eu.org/static/resources/myocean/pum/MYO-INS-PUM-013-v1.0.pdf, and the quality control guidelines by the DBCP http://www.jcommops.org/dbcp/data/qc.html). Moreover, additional quality control (QC) procedures have been applied to all drifter measurements before building our matchup dataset, i.e. a standard outlier detection algorithm that iteratively flags values exceeding five times, four times, and three times the standard deviation error of the difference between satellite and drifters. This last QC procedure eliminates only very evident spikes (about 2% of the total original drifter measurements).

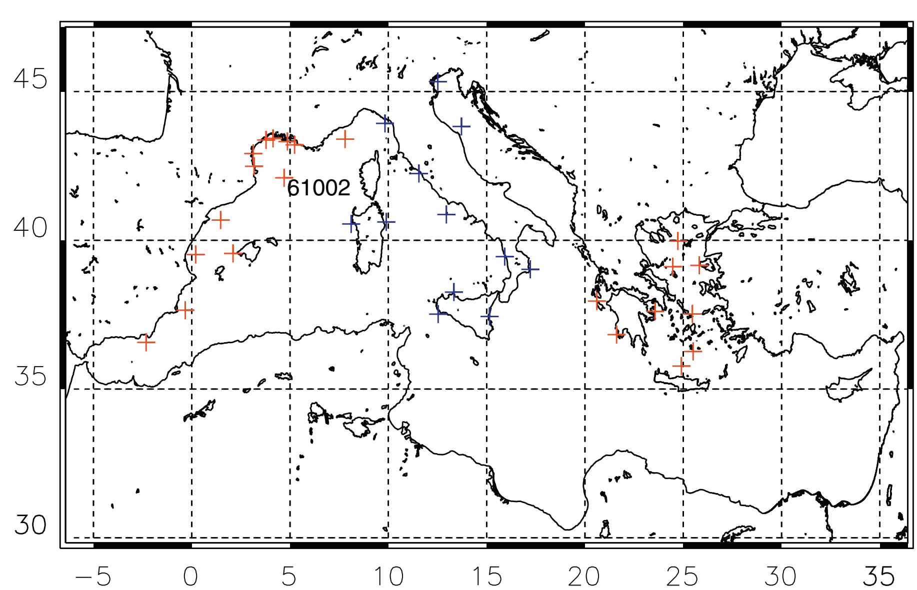

Fig. 1. Map of the Mediterranean moorings used for the validation: MyOcean in situ TAC (red crosses) and ISPRA (blue crosses) networks. The position of mooring 61002 is highlighted.

An hourly matchup database between the operational SEVIRI L3C hourly product, model SST, DOISST and drifter measurements has been compiled keeping the collocated drifter and satellite/model data. Since within 1 h more than one pixel can be visited by a drifter, the hourly matchup string contains the average of drifter measurements acquired during that hour, the average of the SST sensed by SEVIRI in pixels visited by a drifter (a flag if satellite data are not valid), the average of the DOISST pixels, and MFS-SST grid points visited by the drifter.

A similar matchup criterion has been adopted for the moorings.

2.3. Model data

The Mediterranean Forecasting System (Dobricic et al., 2007; Oddo et al., 2009; Pinardi & Coppini, 2010) has been producing every day a ten day velocity field and temperature forecast for the Mediterranean Sea, and analyses every seven days. The analysis quality has been assessed for the past ten years (Tonani et al., 2009) and the RMSE for the SST has been found to have a large seasonal cycle, with maximum values around 1 °C during summer and 0.3 °C during winter, partly ascribable to the inaccuracies of the simulated diurnal cycle for the summer. The numerical model has a horizontal resolution of 1/16 deg. × 1/16 deg and 71 unevenly spaced vertical levels (Oddo et al., 2009). The first three layers of the model are centered at 1.47 m, 4.59 m and 7.95 m, respectively. MFS assimilates sea level anomaly, night time SST, in situ temperature profiles by VOS XBTs, in situ temperature and salinity profiles by ARGO floats and CTD (Dobricic et al., 2007).

The diurnal cycles in the surface heat fluxes and the model SST are produced by the Reed (1977) formula for shortwave radiation and calibrated formulas for long wave net radiation and turbulent fluxes (Bignami, Marullo, Santoleri, & Schiano, 1995; Pettenuzzo, Large, & Pinardi, 2010) obtained using 6-hourly ECMWF surface state analyses and forecasts (among them, winds, air temperature and clouds). Satellite OISST data (night passes only; Buongiorno Nardelli, Tronconi, Pisano, & Santoleri, 2013) are used as a flux correction term for these surface heat fluxes providing a relatively small correction term for the surface fluxes and not considering diurnal warming effects. Thus the daily SST cycle used in this paper is practically all freely simulated by the model interactive surface fluxes, without relevant satellite SST corrections during the day.

3. The new Diurnal Optimal Interpolation SST scheme

The optimal interpolation (OI) (Bretherton, Davis, & Fandry, 1976; Gandin, 1965) scheme used here was originally developed for the AVHRR sensor in the Mediterranean Sea (Santoleri, Marullo, & Böhm, 1991) and then expanded for use with other sensors (Buongiorno Nardelli, Böhm, Tronconi, & Santoleri, 2007; Buongiorno Nardelli et al., 2013; Marullo, Buongiorno Nardelli, Guarracino, & Santoleri, 2007). The adaptation of the scheme to resolve the diurnal cycle using geostationary satellite observations was proposed by Marullo et al. (2010) for the tropical Atlantic. It includes four basic modules: derivation of the covariance/structure function from available satellite data, residual cloudy pixels flagging, influential data selection and first-guess removal. In Marullo et al. (2010) the OI input fields were SEVIRI data acquired at the same time as the interpolation time over a ±5 day window. An example of this scheme is given by the production of the OI map for 12:00 UTC. This approach requires the input SEVIRI data at 12:00 UTC from the same day and the previous and next five days. This approach was chosen to avoid the presence of the diurnal oscillation in the selected influential points for the interpolation.

The approach proposed here is a modification of this scheme with the aim of accounting for the availability of hourly SST (only three hourly SST fields were available in Marullo et al., 2010) and for the typical SST variability scales in the Mediterranean Sea characterized by abrupt SST changes induced by meteorological forcing and frequent occurrence of intense diurnal warming events (Böhm, Marullo, & Santoleri, 1991; Buongiorno Nardelli, Marullo, & Santoleri, 2005; Gentemann et al., 2008; Merchant et al., 2008). The major change is the use of a new type of first-guess. In this Mediterranean SST reconstruction experiment, instead of using daily Reynolds SSTs (Reynolds et al., 2007) as first guess, we used the hourly model SST analysis produced by the Mediterranean Forecasting System (MFS) a component of the MyOcean service (see Section 2.3).

The rationale behind the use of this new first-guess is to produce an anomaly SST field (the variable to be interpolated in space and time by OI) free (or nearly free) of any diurnal cycle. In fact, the presence of a diurnal frequency in the SST measurements can have the consequence that, at each time (t_0), the data acquired a few hours later are less correlated than those acquired at $T = t_o + 24 * n$ (with $n = \pm 1, \pm 2, \ldots$) (Marullo et al., 2010). Mathematically this implies the existence of a 24 h oscillation in the covariance/structure function with relative maxima often higher than values occurring a few hours after the preceding maximum.

In practice the interpolation variable is the anomaly of the satellite-derived SST field with respect to the model analysis, as shown in Fig. 2. In this example, the diurnal signal, present in both satellite and the model temperatures, with an amplitude of about 1 °C is nearly completely removed in the SST anomaly field shown in Fig. 2b. If the model outputs were exactly representing the real world, or at least the same world sensed by SEVIRI, this anomaly would be free from the diurnal cycle (as in Fig. 2b), allowing us to statistically interpolate between data acquired at different times of the day. The efficacy of this statement will be revealed by the temporal structure of the covariance function. This covariance/structure function $F(x,\Delta t)$ for the SST anomaly has been computed from the valid SEVIRI satellite data and then fitted with an analytical function of distance (both in space and time).

The temporal component of the covariance function $f_t(\Delta t)$ has been estimated from the SST data as a function of the time lag Δt (the central red line in Fig. 3a). The resulting fit is given by:

$$f_t(\Delta t) = e^{\left[-\left(\frac{\Delta t}{t_c}\right)^d\right]}. \tag{1}$$

In this case the nonlinear least square fit between the estimated correlations at different time lags gives $t_c = 36$ h and $d = 0.4$.

Fig. 3a (red line) reveals that a residual diurnal oscillation is still present in the time series of the SST anomalies. This results from the concrete possibility of an even small amplitude difference between the SST diurnal cycle deduced from the data and the one estimated by the model. Nevertheless, the amplitude of this 24 hour residual component, as observed in the covariance function (Fig. 3a), is about one order of magnitude smaller than the one obtained by computing the covariance of the SST field minus a constant daily map (black line of Fig. 3a). This constant daily map can be either the mean of the model analysis over one day (as in Fig. 3a black line) or the Reynolds SST of that particular day (Reynolds et al., 2007), as used by Marullo et al. (2010). Fig. 3a (red line) clearly shows that the correlation decreases faster during the first 12 h, reaching the 0.6 value. Then it continues to decrease at a slower rate after this point. This correlation behavior is well represented by an analytical exponential function as defined in Eq. (1). The occurrence of the reduction of the diurnal signal in the temporal covariance function of SST anomaly allowed us to avoid the approach of Marullo et al. (2010), and to use a series of hourly SST anomalies in the OI scheme with a nearly monotonically decreasing covariance function.

Similarly, the spatial component (Fig. 3b) of the covariance function $f_s(x)$ has been estimated from the data. A nonlinear least square

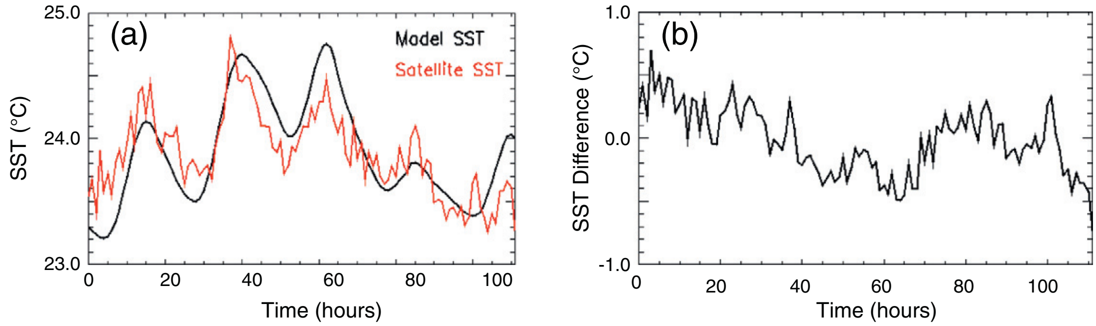

Fig. 2. Example of model first-guess and original SST SEVIRI data over a point in the Mediterranean Sea. (a) Model (black curve) and SEVIRI (red curve) SST time series. (b) Difference between the SEVIRI and model SST.

fit between the estimated correlations and the distances x [km] results in the following expression:

$$f_s(x) = \left[a \cdot e^{-x/b} + \frac{1-a}{(1+x)^c}\right] \tag{2}$$

where $a = 0.70$, $b = 200$ km, and $c = 0.26$.

Finally, the covariance function used in the OI scheme is given by the product of the spatial and the temporal components of the covariance function (i.e., $f_s(x)$ and $f_t(\Delta t)$, respectively):

$$F(x, \Delta t) = f_s(x) \cdot f_t(\Delta t) = \left[a \cdot e^{-x/b} + \frac{1-a}{(1+x)^c}\right] \cdot e^{\left[-\left(\frac{\Delta t}{t_c}\right)^d\right]}. \tag{3}$$

This function has been used in the new DOISST analysis.

The optimal interpolation scheme adopted in this work can be summarized as follows:

1. Hourly SEVIRI SSTs and flags in a time window of ± 24 h around the interpolation time are ingested.
2. Data with quality flag less than 4 are filtered out.
3. Hourly model SSTs are subtracted from valid SSTs (as in Fig. 2) producing SST anomalies.
4. SST anomalies are used as data input for the OI analysis.
5. Optimal interpolation is run using the correlation function defined in Eq. (3).
6. The model SST is added to the OI output again.

The interpolation scheme described above is applied to the 5 km gridded OSI-SAF data to produce complete Diurnal Optimally Interpolated Sea Surface Temperature (DOISST) maps every hour for the summer of 2011.

It is important to underline that subtracting a modeled hourly first-guess from the SST original data produces an hourly anomaly field in which the amplitude of the diurnal signal is minimized and eventually removed. This allows one to reduce the searching window to ± 1 day instead of ± 5 days which is previously used by Marullo et al. (2010). This reduction of the searching window is crucial for regions like the Mediterranean Sea, where the SST field is characterized by a seasonal signal with an amplitude of the order of 20 °C and rapid passage of strong meteorological perturbations that can induce abrupt changes of the SST field.

Fig. 4 shows an example of the SST field reconstruction during a summer day of July 2011, characterized by a particularly intense diurnal warming event. The input satellite SST images at 04:00 and 14:00 UTC show an area of missing data that covers a large portion of the Western Mediterranean basin. An intense diurnal warming event is visible in the southeastern corner of the Tyrrhenian Sea where the temperature at 14:00 UTC reaches values of the order of 30 °C, more than 5 °C greater than the value at 04:00 UTC. In the same region the model analysis shows only an excursion of 1 °C. Other diurnal warming regions are visible in a circular sector from the Southern Adriatic Sea to Tunisia, south of Crete and in the north-western corner of the Aegean Sea. All these events do not present a signature in the model analysis. In this case the OI scheme was able to reconstruct the SST field quite well, i.e. including the diurnal warming event, as well as recovering the deficiency of the model in reproducing extreme warming events. A more quantitative description of the comparison between model, SEVIRI, and in situ data will be given in the next section.

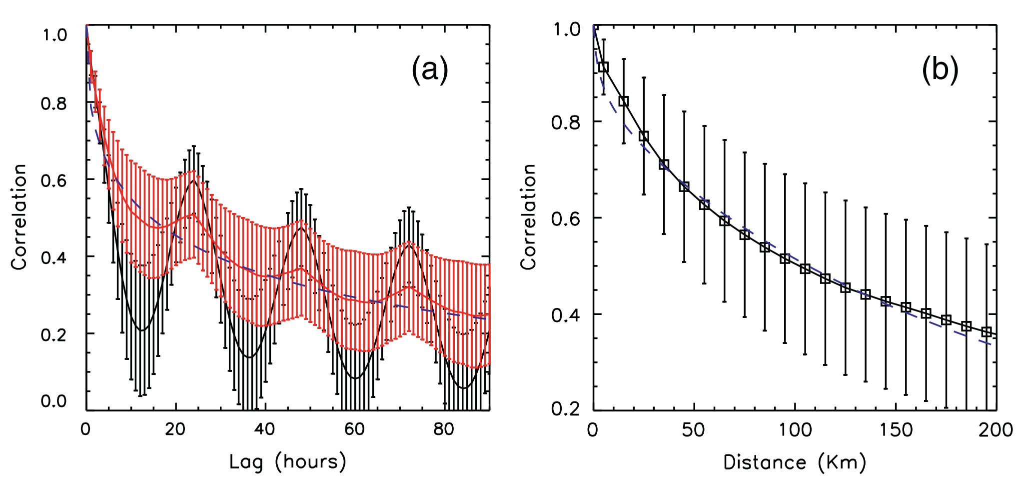

Fig. 3. Covariance structure function of the Mediterranean Sea estimated from summer 2011 SEVIRI data. (a) Temporal covariance: in red the covariance is computed using hourly SST anomaly field (hourly SEVIRI–hourly MFS); in black the covariance is obtained using hourly SST field after removal of mean daily SST (hourly SEVIRI–mean daily MFS). Vertical bars represent ± 1 standard deviation. (b) Spatial covariance function at $\Delta t = 0$ for the SST anomaly field. Dotted blue curves in (a) and (b) represent Eqs. (1) and (2) respectively.

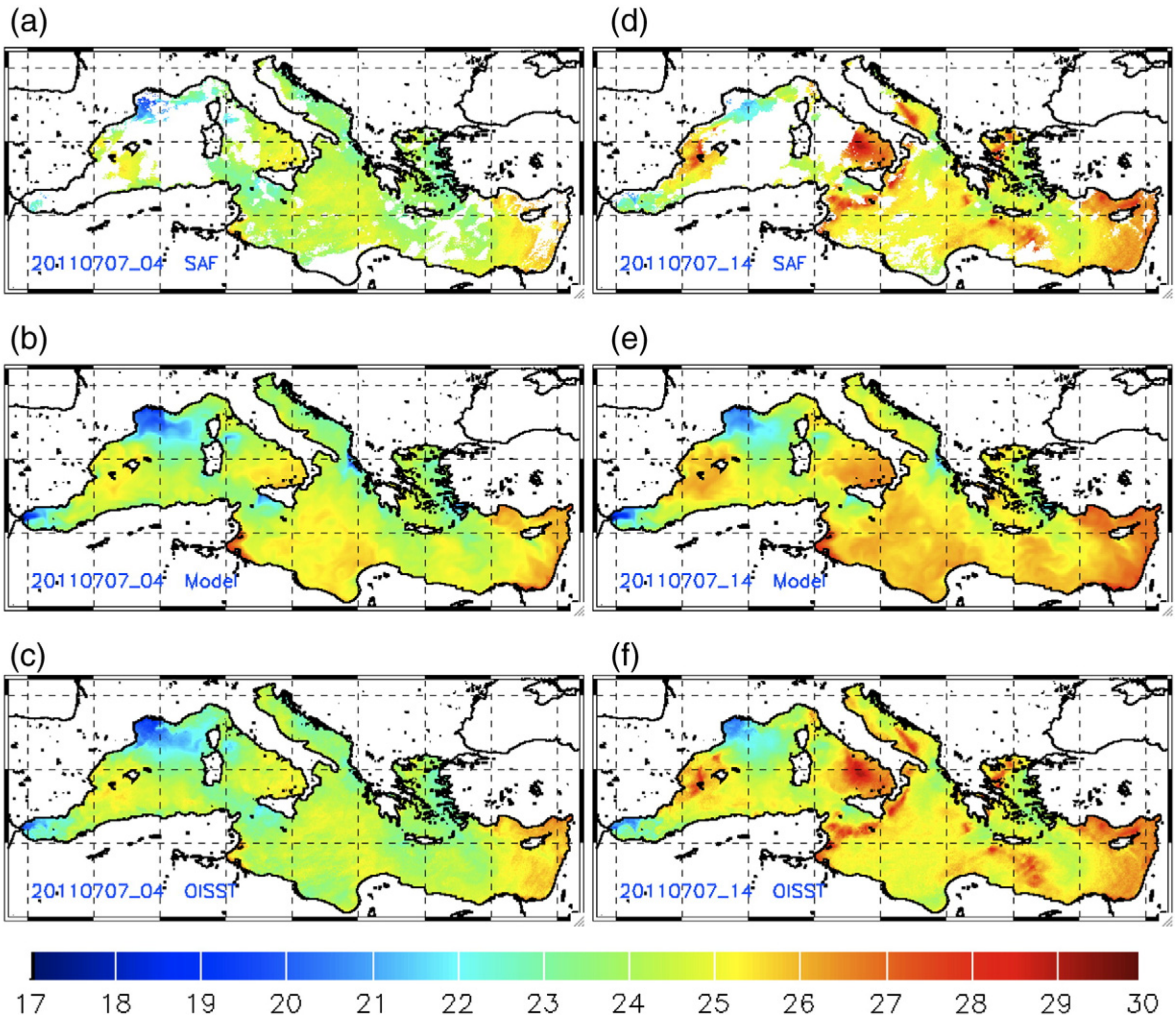

Fig. 4. The SST field on July 7th 2011 at 04:00 (left column) and 14:00 UTC (right column). Original SEVIRI SST (a and d), model first-guess (b and e) and reconstructed SST field (c and f). Units are degree Celsius.

4. Satellite data evaluation

The objective of this section is to demonstrate that SEVIRI data are accurate and frequent enough to reconstruct the diurnal cycle, including diurnal warming events. We here evaluate the goodness of the DOISST products by comparing DOISST either with purposely unused satellite observations or with in situ data.

Having only in situ bulk temperature measurements instead of skin SST, the expected value of the bias between satellite estimates of the skin SST and in situ SSTs should not be zero and the amplitude of their diurnal oscillation is expected to differ.

4.1. SST reconstruction under artificial clouds

Artificial clouds were used to remove part of the SEVIRI observations over different locations of the Mediterranean Sea. Artificial clouds consist of a 200 km wide band that mask all the pixels from the southern to the northern limit of the SEVIRI image. The band moves from the eastern to the western boundary of the Mediterranean Sea in 24 h. The dimension and the starting point of the band were selected in order to avoid that the same pixel is always masked at the same time of the day. In other words the band is shifting its central position so that after 24 h the band does not exactly cover again the same region of the image. This provides a new synthetic SEVIRI time series to be used as an input for the OI scheme and a reference unused satellite

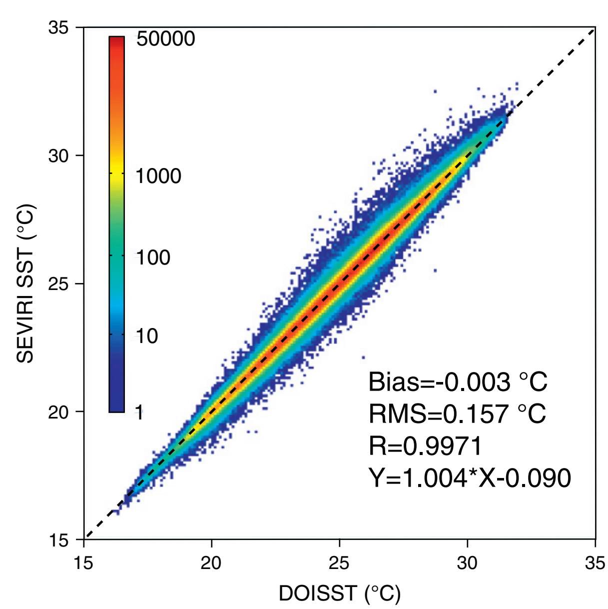

Fig. 5. Scatter plot between SSTs measured by SEVIRI under artificial clouds and reconstructed SST values produced by DOISST.

dataset, that includes all the SEVIRI observations falling under the artificial clouds, to be considered as true value.

This masking procedure has been applied to the entire SEVIRI dataset from 1 June to 31 August 2011. The new masked SEVIRI data are then used as input to the OI scheme described in Section 3 to produce a new time series of DOISST output.

Fig. 5 shows the scatter plot between the DOISST as computed over the pixels masked by the artificial clouds and the corresponding SSTs as measured by SEVIRI. The DOISST estimations are evenly distributed around the line of perfect agreement with a relatively small dispersion. The overall statistics resulting from the comparison between interpolated data and unused SEVIRI observations (6,858,271 matchups) result in a nearly zero bias (0.003 °C), a RMS of 0.16 °C and correlation coefficient of 0.9971, demonstrating the efficacy of the interpolation scheme.

4.2. Comparison with moored buoys

To evaluate whether the SEVIRI sampling was frequent enough to reconstruct the diurnal cycle during the summer of 2011, we compared hourly moored buoy measurements over fixed positions with corresponding reconstructed Optimally Interpolated SSTs (see Section 3), the SEVIRI input data, and MFS model output SST analysis. Table 1 summarizes the basic statistical parameters of the differences between model, SEVIRI valid pixel, SEVIRI interpolated pixel estimates, and buoy measurements. Model SST outputs are generally in agreement with in situ data even if the bias and RMS values are often larger than those obtained using satellite observations.

As it is well known that SST estimation from satellite data is more problematic when approaching a coast, we analyzed the results according to the distance from coastlines.

Standard deviations (RMS) for pixels closer than about 15 NM from the coast range between 0.4 and 1.8 °C with an average value of 1.2 °C both for SEVIRI input data and reconstructed SST fields. On the other hand when the comparison is limited to offshore moorings (>15 NM from the coast) the RMS ranges between 0.5 and 0.8 °C for SEVIRI data and 0.45 to 0.75 °C for DOISST reconstructed fields, with an average value of 0.6–0.7 °C for both satellite and model SST. This clearly indicates that both satellite and model estimates suffer in proximity of the coast.

This is confirmed by the analysis of the bias. In fact, for the same distance intervals, interpolated field bias absolute values range between 0.0 and 1.9 °C in coastal regions and between 0.0 and 0.6 °C in the open ocean. The comparison with the corresponding statistics of input SEVIRI data indicates that the DOISST method performs rather well. The distribution of the statistical parameters resulting from Table 1 suggests that the proximity to the coast can, in some cases, play a role in contaminating the radiation sensed by the satellite sensor with some land contribution and, consequently, distorting the SST estimates and thus the SST reconstruction. The overall analysis of the difference between satellite and mooring data as a function of the distance from the coast, reveals a decrease of the RMS from 1.1–1.3 °C to 0.5–0.7 °C only after 10 NM, i.e. the effect of the coast seems to disappear at distances greater than 3 pixels (i.e. about 15 km).

The overall difference between the satellite (valid pixels) and mooring temperature is −0.15 °C (Table 2). Since SAF produces a subskin

Table 1
Validation of model, SEVIRI and DOISST against moorings. Biases and RMS are in °C. Latitudes and longitudes are in degrees, depths are in m. SURF indicates that the exact depth of the temperature sensor is not available (or is set to zero) in the data files. Dist is the distance of the SEVIRI pixel containing the buoy position from the closest land pixel in nautical miles.

MyOcean model				SEVIRI valid pixels				SEVIRI interpolated pixels				Buoy position			
Bias	RMS	R	N	Bias	RMS	R	N	Bias	RMS	R	N	Dep.	Lon	Lat	Dist (NM)
Distance from the coast less than 15 NM															
0.39	0.44	0.9121	1320	0.69	0.86	0.8155	349	0.59	0.64	0.8711	971	SURF	3.168	42.488	3.0
0.11	1.00	0.9264	1887	0.26	0.80	0.9321	495	0.56	1.12	0.9193	1392	SURF	3.780	43.372	3.0
0.81	1.59	0.8937	1354	1.80	1.81	0.8837	476	1.86	1.50	0.8949	878	SURF	4.866	43.319	3.0
−0.46	1.08	0.7505	674	0.43	0.73	0.8645	381	0.62	0.65	0.9065	293	3	25.815	39.159	3.0
−0.19	0.75	0.9322	1968	−0.80	0.92	0.8895	1523	−1.01	0.96	0.9451	445	0.5	15.147	37.440	3.0
−0.32	0.81	0.8999	1685	−0.70	0.77	0.8797	312	−0.12	0.93	0.8756	1373	0.5	15.917	39.451	3.0
0.06	0.40	0.9751	1975	−0.12	0.51	0.9397	1123	−0.05	0.46	0.9769	852	0.5	17.378	40.975	3.0
0.04	0.94	0.8639	1935	−0.25	1.33	0.7509	1430	−0.44	1.30	0.8365	505	0.5	13.333	38.258	3.0
−0.06	0.93	0.9392	1667	0.10	0.68	0.9695	255	0.41	1.06	0.9271	1412	SURF	4.133	43.425	4.2
−1.53	1.32	0.8108	666	−0.19	0.54	0.9382	551	−0.74	0.63	0.9469	115	1	21.608	36.829	4.2
0.68	0.56	0.9577	673	0.45	0.53	0.9524	569	0.60	0.45	0.9718	104	3	25.462	37.523	4.2
−0.51	0.67	0.9281	1425	−0.23	0.61	0.9073	948	−0.07	0.71	0.9134	477	0.5	8.107	40.549	4.2
−0.04	0.45	0.9672	1971	−0.33	0.49	0.9448	1384	−0.35	0.61	0.9665	587	0.5	17.220	39.024	4.2
0.61	0.70	0.8040	1358	0.24	0.54	0.8761	451	0.64	0.82	0.7524	907	SURF	3.125	42.916	6.7
−1.40	0.49	0.9299	674	−1.43	0.45	0.9408	624	−1.40	0.48	0.9308	50	3	25.501	36.262	6.7
0.94	1.15	0.8883	672	0.81	1.06	0.8693	593	1.43	1.73	0.8766	79	3	23.569	37.610	6.7
0.33	0.65	0.8948	670	0.33	0.62	0.9022	590	−0.15	0.64	0.9109	80	3	20.604	37.956	6.7
−1.55	0.97	0.8362	1942	−1.58	0.97	0.8188	1421	−1.29	0.86	0.8863	521	0.5	11.554	42.245	6.7
−1.31	1.39	0.6645	729	−2.17	1.46	0.6376	503	−1.85	0.86	0.7533	226	0.5	9.892	40.617	6.7
0.25	1.18	0.8660	1926	0.55	0.81	0.9427	1310	1.04	1.34	0.7467	616	0.5	12.533	37.518	8.5
−1.03	1.25	0.9158	1043	0.47	0.61	0.9715	148	−0.03	1.01	0.9429	895	SURF	5.230	43.208	9.0
0.02	0.61	0.9240	1960	−0.19	0.61	0.9058	977	−0.24	0.70	0.9143	983	0.5	9.828	43.929	9.0
0.39	0.79	0.9096	1959	0.60	1.12	0.8326	967	0.38	0.82	0.9108	992	0.5	12.517	45.334	9.0
−0.38	0.74	0.9288	674	0.13	0.65	0.9315	571	0.28	0.79	0.8999	103	3	24.464	39.113	12.0
0.79	0.68	0.9814	616	0.13	0.50	0.9743	298	0.49	0.81	0.9637	318	SURF	−2.320	36.570	12.7
−0.25	0.81	0.9017	1963	−0.08	0.88	0.8318	1045	−0.46	0.72	0.9342	918	0.5	13.719	43.825	15.0
Distance from the coast greater than 15 NM															
0.12	0.48	0.9692	2051	−0.17	0.52	0.9557	1156	−0.22	0.46	0.9775	895	SURF	2.100	39.560	18.0
−0.27	0.98	0.8258	664	−0.19	0.74	0.8590	532	−0.23	0.75	0.8777	132	1	24.724	39.974	21.0
−0.63	0.50	0.9627	1692	−0.52	0.59	0.9124	1021	−0.60	0.57	0.9550	671	0.5	12.950	40.867	22.8
0.28	0.60	0.9401	1386	0.34	0.81	0.8827	714	0.32	0.67	0.9077	672	SURF	7.800	43.400	24.2
−0.10	0.47	0.9657	2054	−0.15	0.64	0.9202	1062	−0.25	0.57	0.9607	992	SURF	0.200	39.520	27.7
−0.19	0.41	0.9498	1856	−0.29	0.62	0.8943	1346	−0.52	0.61	0.9248	510	SURF	−0.330	37.650	29.7
0.57	0.56	0.9547	2058	0.17	0.74	0.9059	974	0.15	0.63	0.9496	1084	SURF	1.470	40.680	31.9
−0.35	0.58	0.9648	2052	0.14	0.56	0.9540	992	−0.01	0.45	0.9838	1060	1	4.700	42.100	85.3

Table 2
Overall statistics of the differences between model, SEVIRI, DOISST and moorings.

	ALL distances				Coastal mooring (<15 NM)				Offshore mooring (>15 NM)			
	Bias	RMS	R	N	Bias	RMS	R	N	Bias	RMS	R	N
Model–mooring	−0.10	0.99	0.9407	49,199	−0.11	1.09	0.9356	35,381	−0.05	0.66	0.9696	13,818
SEVIRI–mooring	−0.15	1.05	0.8981	27,093	−0.17	1.17	0.8826	19,294	−0.11	0.69	0.9473	7799
DOISST–mooring (only interpolated)	−0.08	1.06	0.9408	22,111	0.16	1.18	0.9343	16,092	−0.13	0.64	0.9644	6019
DOISST–mooring (all pixels)	−0.05	1.06	0.9306	49,199	−0.02	1.18	0.9237	35,381	−0.12	0.67	0.9579	13,818

SST, a skin SEVIRI SST can be obtained by subtracting 0.2 °C to SAF SST (see Section 2.1). As a consequence the difference between the SEVIRI skin SST and bulk SST is −0.35 °C, which is slightly larger than the expected skin–bulk daily mean (−0.2 °C, e.g. Webster et al., 1996). This can either be due to the even distribution of the match-up data during a day or to the specific environmental condition that occurred during the investigation period. By computing the statistics including data points reconstructed by interpolation and recovering a uniform distribution of the data during the day, the final value of the difference between satellite SST and bulk buoy measurements becomes −0.05 °C, very close to the expected value for sub-skin SST. To further investigate the impact of using mooring SST for the validation of the satellite product and its diurnal cycle a detailed comparison was performed on buoy #61002 (last row of Table 1) located in the center of the Gulf of Lions (Fig. 1). This mooring was selected among those provided by the MyOcean in situ TAC, because it provides the most offshore observations with hourly sampling at a well known depth (the temperature sensor is located at 1 m depth).

Fig. 6 shows the SST time series for the period June to August 2011 as seen by the buoy, SEVIRI, and the reconstructed SST. Apart from a few spikes observed in SEVIRI and DOISST, the three time series are qualitatively coherent and all three exhibit an evident diurnal signal.

The mean diurnal cycle estimated by DOISST at the mooring location was then compared with the buoy observations. We used the formulation of Zeng et al. (1999) to infer hourly skin SST from hourly buoy bulk SST. The wind data measured at the buoy were used to compute the adjustment. These winds were converted to that at 10 meter height under a neutral condition hypothesis. Subskin SEVIRI data were reconverted to skin temperature by subtracting 0.2 °C (see Section 2.1) to the SAF data. Fig. 7 shows that the diurnal cycle measured by the buoy before the adjustment, has an amplitude similar to that of model even if the model SST, representing the average value over the first 3 m of water column, is cooler than in situ measurements (bias = −0.35 °C). As expected, the amplitude of the satellite skin SST diurnal cycle is much larger (~0.65 C) than that observed by the buoy and the model (~0.45 °C). The satellite temperature has its minimum around 4:00–5:00 LST and reaches its maximum at 17:00 LST while buoy SST has its minimum at 7:00–8:00 LST and reaches its maximum at 17:00 LST. After the adjustment of buoy data (at 1 m depth) to the skin level the mean daily bias between satellite and buoy temperatures approaches zero, the two amplitudes become comparable even though the delay of the buoy measurement with respect to the satellite estimate is not recovered. The delay of the temperature signal at 1 m depth with respect to the skin level, during the warming and the cooling phase, indicates that the heat transfer in the water column is a more complex process than the one described by a simplified wind-based empirical model.

The relative importance of the diurnal oscillation in the buoy and in the reconstructed DOISST time series can be evaluated by investigating the spectral characteristics of the two time series (buoy and DOISST) and of the model time series used as first guess for the DOISST. To investigate the consistency of the high-frequency variability in the model, buoy, and reconstructed time series we performed a spectral analysis applying the Multitaper method to the detrended time series of Fig. 8. Following Ghil et al. (2002) we set the number of tapers k to 3 and the bandwidth parameter p to 2.

Two of the three spectra (Fig. 8a and b) show the presence of an evident peak at 24 h well above the 99% confidence limit and several higher frequency peaks between 5 and 2 h just above the same confidence limit. Differently from the first two (buoy and DOISST) the model spectrum only has two prominent peaks above the 99% confidence limit at 24 and 12 h, respectively, going below the red noise background level for periods shorter than half a day.

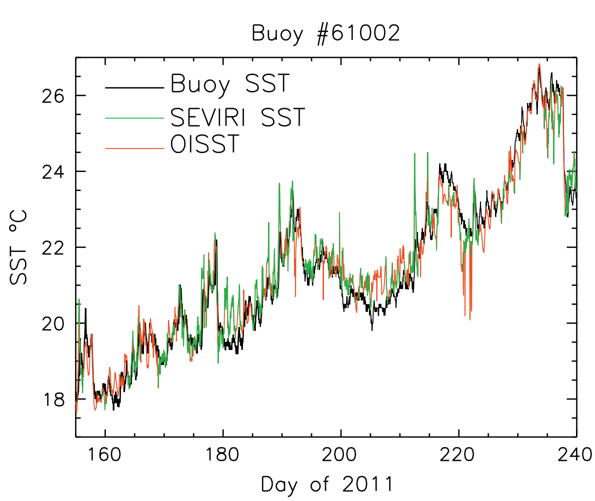

Fig. 6. Sea Surface Temperature time series at buoy 61002 from SEVIRI (green), OISST (red) and buoy sensor (black).

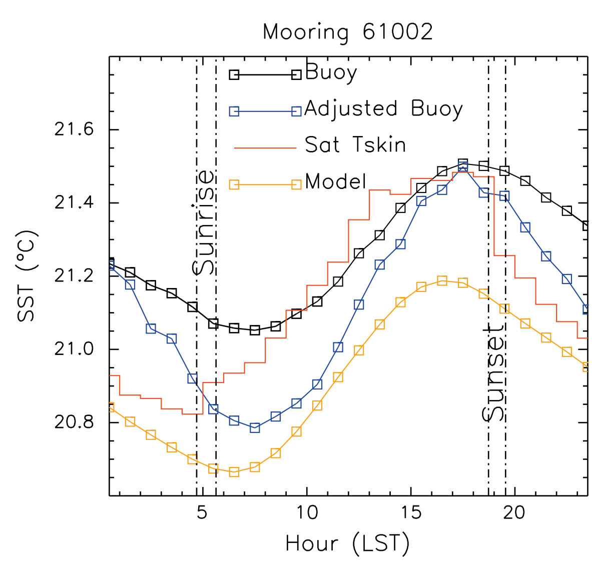

Fig. 7. Mean diurnal SST cycle measured at mooring 61002 in the Gulf of Lyons. DOISST satellite skin temperature (SAF −0.2 °C) in red, buoy SST measured at 1 meter depth (in black), buoy measurements adjusted to the skin level using Zeng et al. (1999) (in blue), first layer model SST (centered at 1.47 m) in yellow. The two vertical bands represent the sunrise and sunset time limits during the investigation period from Jun 1st to August 31st.

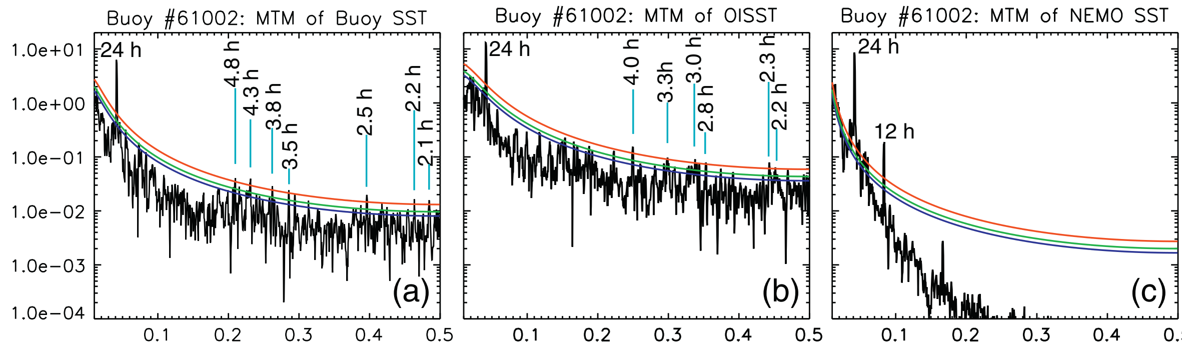

Fig. 8. MTM spectrum of the de-trended sea surface temperature measured by buoy (a), DOISST (b) and MFS (c). The associated 90%, 95% and 99% significance levels are shown by the three smooth curves in blue, green and red respectively. The bandwidth parameter $p = 2$, and $k = 3$ tapers were used. Periods that pass the 99% confidence limit are also indicated.

The most evident difference between the satellite reconstruction and the buoy power spectrum $p(f)$ is the level of the red noise background that is much higher in the satellite reconstructions, reflecting the different nature of the two measurements. In fact, considering that the power spectrum $p(f)df$ can be interpreted as an approximate measure of the variance of the process in the frequency range between f and $f + df$, it follows that the noise level differences between the two spectra can be considered as the consequence of the noise filtering produced by the deeper measure of the buoy (1 m depth) with respect to the skin satellite measurement.

This analysis confirms that the reconstruction, based on SEVIRI data, is able to capture the daily cycle with significance comparable with that observed by the buoy sensor. The reconstruction also reproduces higher frequency oscillations with periods similar to those seen by the buoy. The optimal analysis reconstruction preserves the spectral characteristics of the original SEVIRI time series recovering higher frequencies not present in the model first guess.

4.3. Comparison with drifters

4.3.1. The mean diurnal cycle

Compared to the moored measurements, the drifting buoys provide SST data farther from the coast and at shallower depths (about 20 cm). At this depth the temperature measured by a sensor should be closer to that sensed by satellite even though the two diurnal cycles can still differ.

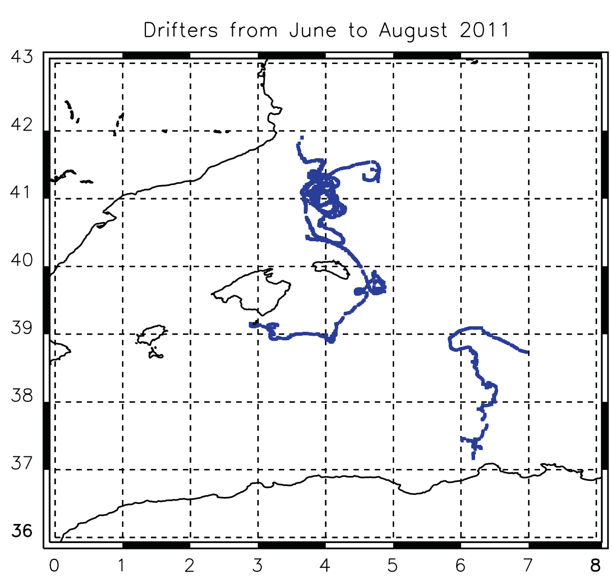

Fig. 9. Position of the drifter matchups from June to August 2011.

Fig. 9 shows the positions of the satellite matchup points with drifter measurements during the investigation period. The basic statistics of the comparison between SEVIRI, DOISST, model, and drifter SSTs are given in Tables 3 and 4 for measured and reconstructed pixels respectively. On the average, the model analysis overestimates drifter SST by 2 tenths of degree with a standard deviation of about 0.6 °C and a correlation coefficient between 0.95 and 0.97 for both valid and interpolated pixels. Satellite SST, on the contrary, underestimate the drifters by 0.16 °C over valid pixels while the bias approaches zero for DOISST interpolated values. The standard deviation is more or less the same, close to 0.5 °C with comparable correlation coefficients (0.97).

Results of this analysis confirm that the interpolation procedure does not significantly change the basic statistical properties of the difference between in situ and satellite measurements.

By having demonstrated that in situ measurements and satellite data both contain a diurnal signal (Section 4.2), the next question to answer is whether drifter, model, SEVIRI, and DOISST SST data describe the same diurnal cycle. A first answer can be obtained by comparing the mean diurnal cycle by binning all the data at hourly intervals (local time) over the matched-up points (Fig. 10).

All the three SSTs peak between 15:00 and 16:00 LST. The amplitude of the SEVIRI and drifter SST diurnal cycles is approximately the same (~1.2 °C, see Fig. 10b).

The application of the Zeng et al. (1999) model to the range of conditions that occur in the Mediterranean Sea during the investigation period predicts a reduction of the diurnal cycle amplitude between the skin-layer and 20 cm of depth of about 10%. In our case this implies a difference between the satellite and drifter diurnal cycle amplitude of about 0.1 °C consistent with our findings (Fig. 10). The bias between SEVIRI and drifter SST is nearly constant (−0.15 °C) as already indicated by the basic statistical parameters in Table 3. This agreement is a confirmation of the findings by Le Borgne, Legendre, and Péré (2012) over the entire SEVIRI disk. The model cycle, on the contrary, shows a reduced amplitude (~1 °C) with a positive bias of about 0.2 °C before 10:00 and after 17:00 LST.

If the comparison between SEVIRI and the model SST is extended to satellite valid pixels over the entire Mediterranean basin (Fig. 11a), a second effect clearly appears. On the average, the model underestimates the SEVIRI diurnal cycle amplitude by about 0.2–0.3 °C. Also, the model SST seems to be delayed with respect to the satellite SST by about 2 h (Fig. 11a), as already observed at the mooring location (Fig. 7a). The

Table 3
Model minus drifters and SEVIRI minus drifters' mean biases, standard deviation, correlation coefficient and number of data points (valid pixels only).

	Bias	RMS	R	N
Model − drifters	0.20	0.59	0.9575	2223
SEVIRI − drifters	−0.16	0.47	0.9742	2223

Table 4
Model minus drifters and DOISST minus drifters' mean biases, standard deviation, correlation coefficient and number of data points (reconstructed pixels only).

	Bias	RMS	R	N
Model − drifters	0.25	0.60	0.9684	1748
DOISST − drifters	−0.07	0.56	0.9732	1748

same conclusion is reached if we extend the model comparison over the entire Mediterranean Sea pixels using the reconstructed DOISST field (Fig. 11b). We can qualitatively interpret this delay as the physical result of delayed solar heating of the first model layer (centered at about 1.5 m) and of the skin layer sensed by the satellite. Also this may be a consequence of the different packaging of the SEVIRI and model SST data in to the hourly files. For example the model hourly SST at 12:00 is the mean value of the analysis between 12:00 and 12:59, while SAF SEVIRI SST at 12:00 is the best SST (in terms of quality flags) measured within a time interval of 1 h centered over 12:00 (11:30–12:29).

4.3.2. Diurnal warming events

This section is focused on the evaluation of the capability of model and satellite OI reconstructed SST estimates to capture diurnal warming (DW) events over the Mediterranean Sea. The diurnal warming is defined as the difference between the surface temperature at a given location minus the foundation SST, the latter being defined as the temperature of the water column just below the diurnal warm layer, free of diurnal temperature variability or equivalently the temperature at the first time of the day when the heat gain from the solar radiation absorption exceeds the heat loss at the sea surface (see GHRSST definition at https://www.ghrsst.org/ghrsst-science/sst-definitions/). Our evaluation has been performed by analyzing the DW signal observed by drifters, by SEVIRI original data, and by DOISST and model fields. From a satellite point of view, which experiences the presence of data voids due to cloud cover, DW can be equivalently defined as the hourly SST measured during daytime minus the mean of the previous night-time SST. The latter temperature can be defined as the mean of all the valid SST measurements between midnight and the time when the solar zenith angle becomes less than 90°. We applied this definition to our SEVIRI dataset and to the corresponding DOISST and model temperatures. We then compared these DW estimates with corresponding DW observed in the drifters (Fig. 12).

The scatter plot between SEVIRI and buoy DW data (Fig. 12 a) shows a good agreement between satellite and in situ measurements as confirmed by low bias (0.03 °C), a small RMS (0.4) and high correlation coefficient (0.85). The DW signal reaches values as high as 3 °C in both buoys and satellite measurements. When we compare the DW signal observed in our SST reconstructed field (using only reconstructed pixels) the scatter plot with in situ measurements (Fig. 12b) is still uniformly distributed around the perfect agreement line, although a slightly higher dispersion of data is observed. Nevertheless, the bias and standard deviation remain very close to those of the measured data. This implies that DOISST is able to capture the DW signal as well as the original SEVIRI data.

The difference between the range of DW variability observed from satellite or from drifters and the variability estimated from the model appears evident comparing Fig. 12c and d. In general model analysis is not able to reproduce DW values exceeding 1.4 °C. This different behavior could be justified by the different quantities measured by the drifters and satellite once compared to what is simulated by the model. In fact, while the satellite and the drifters measure the skin and the 20 cm depth temperature, the first layer of the model simulates the average temperature of the top 3 m of the ocean.

If we suppose that the first model layer temperature is only driven by heat fluxes the depth integrated equation, describing the local time rate of temperature change, is given by:

$$\rho_0 C_p h \frac{\partial T}{\partial t} = Q_0 - Q_{-h} \tag{4}$$

where $\rho_0 \approx 1027$ kg m^{-3} is the sea water density, $C_p = 3.94 \times 10^3$ J kg^{-1} K^{-1} is the heat capacity at constant pressure, $h = 3$ m is the thickness of the first model layer, T is the average water temperature of the first layer, t is the time, Q_0 is the surface heat flux and Q_{-h} represents the sum of the heat flux due to penetrative short wave radiation and turbulent mixing at the base of the upper layer. An upper bound for the variation of the temperature during the heating phase of the day can be estimated by supposing null fluxes at the lower boundary of the water column, which implies that only surface heating is acting to produce a diurnal increase of the sea temperature. An upper bound for a summer diurnal warming event can be estimated by selecting a day and an area of the Mediterranean Sea where the ocean heat gain during day time was particularly intense. On 7th July in the southern Tyrrhenian Sea (Fig. 4) the mean heat gain was about 500 W m^{-2}. This implies (Eq. 4) an upper bound for the diurnal warming of about 1.8 °C. This value is slightly greater than the highest DW values of Fig. 12d, but significantly lower than the drifter and satellite DWs.

In the real world, other factors – in addition to the air–sea heat fluxes – play a role: horizontal advection, which we neglected for our

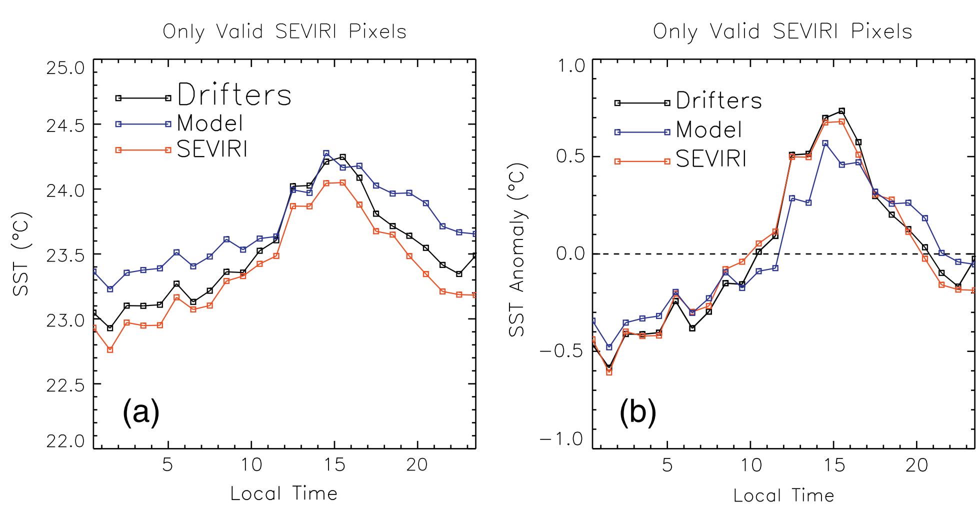

Fig. 10. Comparison between the mean diurnal cycle observed by satellite, model and drifters. Mean hourly SST values from SEVIRI valid data (red), model (blue) and drifters (black) computed using all the satellite-in situ match-up points (a). Mean SST anomalies obtained from the three curves in Fig. 8a after removal of the mean daily value (b).

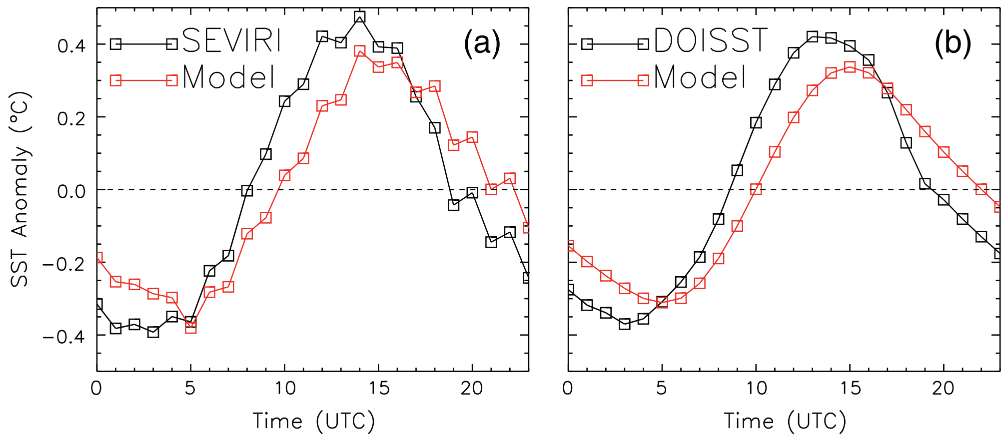

Fig. 11. (a) Comparison between SEVIRI and model mean diurnal cycle over the entire Mediterranean Sea from June to August 2011 using valid pixels only. (b) Comparison between DOISST and model diurnal cycle over the entire Mediterranean Sea. Units are degree Celsius.

specific analysis; vertical mixing, that recalls colder deeper waters toward the sea surface; entrainment at the base of the upper layer that is the major contribution to the Q_{-h} term in Eq. (4) (actually fixed to zero); eddy components and, last but not the least, the penetration of the solar radiation below the base of the surface layer. All these terms together can largely justify the rare presence of DW values greater than 1 °C in the DW model estimates.

5. Conclusions

In this paper we presented a new OI analysis scheme to reconstruct the hourly SST field from geostationary satellite data (DOISST). The proposed scheme uses a new first guess based on the SST field simulated by the Mediterranean Forecasting System (MFS). This allows one to calculate an hourly anomaly SST field that produces a reduction of the diurnal

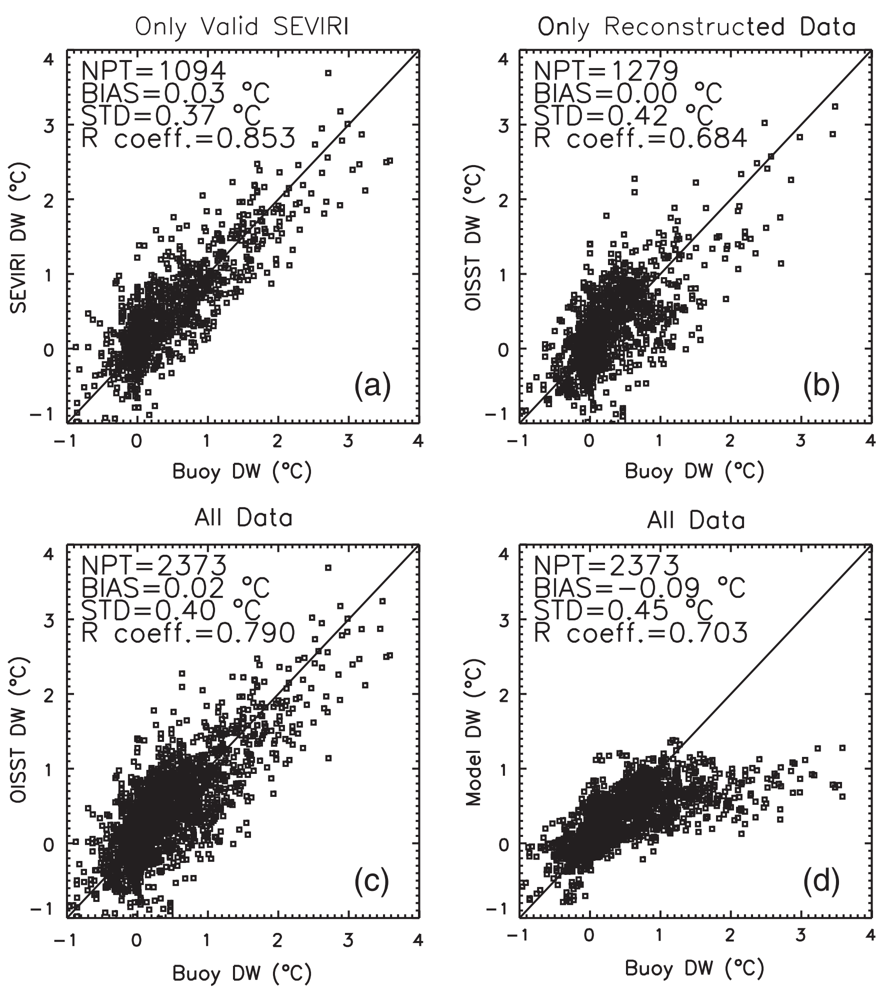

Fig. 12. Analysis of the DW in SEVIRI, DOISST, model and drifter data. (a) SEVIRI versus drifters, (b) DOISST reconstructed pixels versus drifters, (c) DOISST (all pixels: measured and reconstructed) versus drifters, (d) model DW versus drifters' DW.

oscillation in the temporal covariance of about an order of magnitude (Fig. 3a) with respect to the full signal. This reduction allows one to interpolate the hourly SST field using input data acquired at different times of the day. As a further consequence, the new hourly OI scheme allows one to reduce to 1 day the temporal window for the selection of the pertinent data used by the interpolation (at least for the period of investigation), instead of the 5 days used by Marullo et al. (2010).

The evaluation of the DOISST products demonstrates that the reconstructed SST is relatively accurate when compared to in situ data, and correctly reproduces the diurnal variability in the Mediterranean Sea.

The statistical properties obtained by comparing SEVIRI input data with in situ measurements (see Table 3) are similar to those obtained by comparing the DOISST reconstructed field with the same reference dataset (see Tables 2 and 4). The evaluation of DOISST products against drifter measurements results in a mean bias of −0.07 °C and a RMS error of 0.56 °C. These values are comparable with the recent validation results obtained by Buongiorno Nardelli et al. (2013) for daily L4 Mediterranean operational SST products covering the period 2010–2011 (Bias = −0.1, RMS = 0.52 °C) which do not resolve the diurnal cycle. Note that while our bias and RMS estimates only refer to interpolated data points the Buongiorno Nardelli et al. (2013) estimates refer to the entire OI field, which includes both interpolated and measured SSTs.

The comparison between mooring measurements and satellite data shows that particular attention must be devoted to the selection of the matchup, taking into account the distance from the coast, the depth of the temperature sensors, and the quality control of the diurnal cycle detected by the moorings. The use of drifters with temperature sensors at about 20 cm is highly recommended, along with a careful quality control of the data, when radiometric in situ temperature data are not available.

The analysis of the diurnal cycle, detected by SEVIRI, DOISST, model, and in situ measurements in the Gulf of Lyons mooring station, allowed us to investigate the physical meaning of the differences between in situ bulk observations and satellite estimates. It results that part of the mean bias between temperature measured at 1 m depth and the satellite observation can be ascribed to the different nature of the measurements (bulk versus skin). The different amplitude of the diurnal cycle measured by satellite and by the mooring sensor is consistent with the physical consequence of the vertical heat transfer process occurring in the upper ocean, which implies a decrease of the diurnal wave temperature with depth. The adjustment of the buoy measurements to the skin level allows recovering the amplitude of the diurnal cycle sensed by SEVIRI even though a delay of about 2–3 h with respect to the satellite observation is still present (Fig. 7). The satellite DOISST, after reaching its minimum, starts to increase again between 5 and 6 LST just after the sunrise while the adjusted buoy SST starts to increase 2–3 h later. The SST maximum is observed around 17 LST for both DOISST and in situ temperature. The different time evolution of the two diurnal cycles should be investigated by considering all the physical processes which drive the heating and cooling of the upper ocean layer, such as air–sea fluxes, molecular conduction at the air–sea interface, attenuation of the short wave radiation, turbulent mixing, etc. (Castro, Wick, & Emery, 2003; Gentemann, Minnett, & Ward, 2009; Zeng & Beljaars, 2005).

Finally, the use of artificially simulated clouds allows the demonstration of the capability of DOISST to correctly reconstruct the SST field. SEVIRI observations obscured by artificial clouds and corresponding OI reconstruction are unbiased and uniformly distributed around the line of perfect agreement with a RMS of 0.16 °C and correlation coefficient of 0.9971. The validation of the reconstructed diurnal cycle shows that the DOISST is able to reproduce the DW events and preserves both statistical and spectral characteristics of the measured SEVIRI field (as seen in Fig. 4 and 12). The spectral analysis of the SST time series (Fig. 8) confirms that DOISST, SEVIRI SST, and model SST have the same evident and significant peak at 24 h. Moreover, sub-daily frequencies observed by in situ SST are well represented in the DOISST spectra even though they are absent in the model first guess, as shown in Fig. 8. This proves that the introduction of the model first guess does not perturb the spectral characteristics of the reconstructed SST field and maintains the quality of the satellite input data.

In the next phase, the method proposed in this study will be implemented in the Mediterranean SST processing chain in order to operationally produce hourly DOISST fields. This will open a new avenue for starting the assimilation of hourly SST interpolated fields in numerical forecasting models.

Acknowledgments

This research was supported by the MyOcean-2 project of the European Union 7th Framework Programme and the Italian RITMARE Flagship Project. The data from the EUMETSAT Satellite Application Facility on Ocean and Sea Ice are accessible through the SAF's homepage: http://www.osi-saf.org.

References

Anding, D., & Kauth, R. (1970). Estimation of sea surface temperature from space. *Remote Sensing of Environment*, *1*, 217–220.

Bernie, D., Guilyardi, E., Madec, G., Slingo, J., & Woolnough, S. (2007). Impact of resolving the diurnal cycle in an ocean–atmosphere GCM: Part 1. A diurnally forced OGCM. *Climate Dynamics*, *29*(6), 575–590.

Bernie, D., Guilyardi, E., Madec, G., Slingo, J., Woolnough, S., & Cole, J. (2008). Impact of resolving the diurnal cycle in an ocean–atmosphere GCM: Part 2. A diurnally coupled OGCM. *Climate Dynamics*, *31*(7–8), 909–925.

Bignami, F., Marullo, S., Santoleri, R., & Schiano, M. E. (1995). Longwave radiation budget in the Mediterranean Sea. *Journal of Geophysical Research*, *100*(C2), 2501–2514.

Böhm, E., Marullo, S., & Santoleri, R. (1991). AVHRR visible-IR detection of diurnal warming events in the western Mediterranean Sea. *International Journal of Remote Sensing*, *12*(4), 695–701.

Bretherton, F. P., Davis, R. E., & Fandry, C. B. (1976). A technique for objective analysis and design of oceanographic experiments applied to MODE-73. *Deep Sea Research*, *23*, 559–582.

Buongiorno Nardelli, B., Böhm, E., Tronconi, C., & Santoleri, R. (2007). *Report on the merging of AVHRR, AATSR and MODIS SST products in the Mediterranean Sea, contract IP3-CT-2003–502885.* Plouzané, France: Mar. Environ. and Security for the Eur. Area Integrated Proj.

Buongiorno Nardelli, B., Marullo, S., & Santoleri, R. (2005). Diurnal variations in AVHRR SST fields: A strategy for removing warm layer effects from daily images. *Remote Sensing of Environment*, *95*(1), 47–56. http://dx.doi.org/10.1016/j.rse.2004.12.005.

Buongiorno Nardelli, B., Tronconi, C., Pisano, A., & Santoleri, R. (2013). High and ultra high resolution processing of satellite sea surface temperature data over the Southern European Seas in the framework of MyOcean project. *Remote Sensing of Environment*, *129*, 1–16.

Casey, K., & Donlon, C.GHRSST Science Team. (2011). The recommended GHRSST data specification (GDS) 2.0, revision 4. [online], 123 pp. https://www.ghrsst.org/documents/q/category/gds-documents/operational/

Castro, S. L., Wick, G. A., & Emery, W. J. (2003). Further refinements to models for the bulk–skin sea surface temperature difference. *Journal of Geophysical Research*, *108*(C12), 3377. http://dx.doi.org/10.1029/2002JC001641.

Chen, S. S., & Houze, R. A., Jr. (1997). Diurnal variation and life-cycle of deep convective systems over the tropical Pacific warm pool. *Quarterly Journal of the Royal Meteorological Society*, *123*, 357–388.

Derrien, M., & Le Gléau, H. (2005). MSG/SEVIRI cloud mask and type from SAFNWC. *International Journal of Remote Sensing*, *26*(21), 4707–4732.

Dobricic, S., Pinardi, N., Adani, M., Tonani, M., Fratianni, C., Bonazzi, A., et al. (2007). Daily oceanographic analyses by the Mediterranean basin scale assimilation system. *Ocean Sciences*, *3*, 149–157.

Embury, O., Merchant, C. J., & Corlett, G. K. (2012). A reprocessing for climate of sea surface temperature from the along-track scanning radiometers: Initial validation, accounting for skin and diurnal variability. *Remote Sensing of Environment*, 62–78. http://dx.doi.org/10.1016/j.rse.2011.02.028.

EUMETSAT (2011). Geostationary sea surface temperature product user manual. SAF/OSI/CDOP/M-F/TEC/MA/181. http://www.osi-saf.org

François, C., Brisson, A., Le Borgne, P., & Marsouin, A. (2002). Definition of a radio sounding database for sea surface brightness temperature simulations: Application to sea surface temperature retrieval algorithm determination. *Remote Sensing of Environment*, *81*, 309–326.

Gandin, L. S. (1965). *Objective analysis of meteorological fields.* 242 pp. Jerusalem: Isr. Program for Sci. Transl.

Gentemann, C. L., & Minnett, P. J. (2008). Radiometric measurements of ocean surface thermal variability. *Journal of Geophysical Research*, *113*, C08017. http://dx.doi.org/10.1029/2007JC004540.

Gentemann, C. L., Minnett, P. J., Le Borgne, P., & Merchant, C. J. (2008). Multi-satellite measurements of large diurnal warming events. *Geophysical Research Letters*, *35*, L22602. http://dx.doi.org/10.1029/2008GL035730.

Gentemann, C. L., Minnett, P. J., & Ward, B. (2009). Profiles of ocean surface heating (POSH): A new model of upper ocean diurnal warming. *Journal of Geophysical Research*, *114*, C07017. http://dx.doi.org/10.1029/2008JC004825.

Ghil, M., Allen, M. R., Dettinger, M.D., Ide, K., Kondrashov, D., Mann, M. E., et al. (2002). Advanced spectral methods for climatic time series. *Reviews of Geophysics*, *40*(1), 1003. http://dx.doi.org/10.1029/2000RG000092.

Intergovernmental Oceanographic Commission (1999). *Global physical ocean observations for GOOS/GCOS: An action plan for existing bodies and mechanisms.* GOOS Rep. 66, GCOS Rep. 51, IOC/INF-1127. Paris, France: UNESCO.

Jessup, A., & Branch, R. (2008). Integrated ocean skin and bulk temperature using the calibrated infrared in situ measurement system (CIRIMS) and through-hull ports. *Journal of Atmospheric and Oceanic Technology*, *25*, 579–597. http://dx.doi.org/10.1175/2007JTECHO479.1.

Kennedy, J. J., Brohan, P., & Tett, S. F. B. (2007). A global climatology of the diurnal variations in sea-surface temperature and implications for MSU temperature trends. *Geophysical Research Letters*, *34*, L05712. http://dx.doi.org/10.1029/2006GL028920.

Le Borgne, P., Legendre, G., & Péré, S. (2012). Comparison of MSG/SEVIRI and drifting buoy diurnal warming estimates. *Remote Sensing of Environment*, *124*, 622–626.

Le Borgne, P., Roquet, H., & Merchant, C. J. (2011). Estimation of sea surface temperature from the spinning enhanced visible and infrared imager, improved using numerical weather prediction. *Remote Sensing of Environment*, *115*, 55–65.

Marullo, S., Buongiorno Nardelli, B., Guarracino, M., & Santoleri, R. (2007). Observing the Mediterranean Sea from space: 21 years of Pathfinder-AVHRR sea surface temperatures (1985 to 2005), re-analysis and validation. *Ocean Science*, *3*, 299–310.

Marullo, S., Santoleri, R., Banzon, V., Evans, R. H., & Guarracino, M. (2010). A diurnal-cycle resolving sea surface temperature product for the tropical Atlantic. *Journal of Geophysical Research*, *115*, C05011. http://dx.doi.org/10.1029/2009JC005466.

Merchant, C. J., Filipiak, M. J., Le Borgne, P., Roquet, H., Autret, E., Piollé, J. -F., et al. (2008). Diurnal warm-layer events in the western Mediterranean and European shelf seas. *Geophysical Research Letters*, *35*, L04601. http://dx.doi.org/10.1029/2007GL033071.

Merchant, C. J., & Le Borgne, P. (2004). Retrieval of sea surface temperature from space based on modeling of infrared radiative transfer: Capabilities and limitations. *Journal of Atmospheric and Oceanic Technology*, *22*(11), 1734–1746.

Minnett, P. J. (2003). Radiometric measurements of the sea-surface skin temperature: The competing roles of the diurnal thermocline and the cool skin. *International Journal of Remote Sensing*, *24*(24), 5033–5047. http://dx.doi.org/10.1080/0143116031000095880.

Nyquist, H. (1924). Certain factors affecting telegraph speed. *Bell System Technical Journal*, *3*, 324–346.

Oddo, P., Adani, M., Pinardi, N., Fratianni, C., Tonani, M., & Pettenuzzo, D. (2009). A nested Atlantic–Mediterranean sea general circulation model for operational forecasting. *Ocean Science*, *5*, 461–473.

Pettenuzzo, D., Large, W. G., & Pinardi, N. (2010). On the corrections of ERA-40 surface flux products consistent with the Mediterranean heat and water budgets and the connection between basin surface total heat flux and NAO. *Journal of Geophysical Research*, *115*, C06022. http://dx.doi.org/10.1029/2009JC005631.

Pinardi, N., & Coppini, G. (2010). Operational oceanography in the Mediterranean Sea: The second stage of development. *Ocean Science*, *6*, 263–267.

Prabhakara, C., Dalu, G., & Kunde, V. G. (1974). Estimation of sea surface temperature from remote sensing in the 11 to 13-μm window region. *Journal of Geophysical Research*, *79*, 5039–5044.

Reed, R. K. (1977). On estimating insolation over the ocean. *Journal of Physical Oceanography*, *7*, 482–485.

Reynolds, R. W., Smith, T. S., Liu, C., Chelton, D. B., Casey, K. S., & Schlax, M. G. (2007). Daily high-resolution-blended analyses for sea surface temperature. *Journal of Climate*, *20*, 5473–5496. http://dx.doi.org/10.1175/2007JCLI1824.1.

Santoleri, R., Marullo, S., & Böhm, E. (1991). An objective analysis scheme for AVHRR imagery. *International Journal of Remote Sensing*, *12*(4), 681–693.

Stommel, H. (1969). Observations of the diurnal thermocline. *Deep Sea Research Part I: Oceanographic Research Paper*, *16*, 269–284.

Stommel, H., & Woodcock, A. H. (1951). Diurnal heating of the surface of the Gulf of Mexico in the spring of 1942. *Eos, Transactions of the American Geophysical Union*, *32*(4), 565–571.

Stuart-Menteth, A.C., Robinson, I. S., & Challenor, P. G. (2003). A global study of diurnal warming using satellite-derived sea surface temperature. *Journal of Geophysical Research*, *108*(3155). http://dx.doi.org/10.1029/2002JC001534 (12 PP.).

Sykes, P., While, J., Sellar, A., & Martin, M. (2011). Diurnal variability in sea surface temperature: Observation and model assessment. *Met Office forecasting research technical report 556*.

Tonani, M., Pinardi, N., Pistoia, J., Dobricic, S., Pensieri, S., de Alfonso, M., et al. (2009). Mediterranean forecasting system: Forecast and analysis assessment through skill scores. *Ocean Science*, *5*, 649–660.

Walton, C. C., Pichel, W. G., Sapper, J. F., & May, D. A. (1998). The development and operational application of nonlinear algorithms for the measurement of sea surface temperatures with the NOAA polar-orbiting environmental satellites. *Journal of Geophysical Research*, *103*, 27,999–28,012.

Webster, P. J., Clayson, C. A., & Curry, J. A. (1996). Clouds, radiation and the diurnal cycle of sea surface temperature in the tropical western pacific. *Journal of climate*, *9*, 1712–1728.

Webster, P. J., & Lukas, R. (1992). TOGA COARE — The coupled ocean and atmosphere response experiment. *Bulletin of the American Meteorological Society*, *73*, 1377–1416.

Zeng, X., & Beljaars, A. (2005). A prognostic scheme of sea surface skin temperature for modeling and data assimilation. *Geophysical Research Letters*, *32*, L14605. http://dx.doi.org/10.1029/2005GL023030.

Zeng, X., & Dickinson, R. E. (1998). Impact of diurnally-varying skin temperature on surface fluxes over the tropical Pacific. *Geophysical Research Letters*, *25*, 1411–1414.

Zeng, X., Zhao, M., Dickinson, R. E., & He, Y. (1999). A multi-year hourly sea surface skin temperature dataset derived from the TOGA TAO bulk temperature and wind speed over the tropical Pacific. *Journal of Geophysical Research*, *104*, 1525–1536.